ORIGINAL RESEARCH

Altered functional connectivity of dentate nucleus in parkinsonian and cerebellar variants of multiple system atrophy

HuaGuang Yang[1] · Na Wang[1] · XiaoGuang Luo[2] · Hong Lv[2] · Hu Liu[1] · GuoGuang Fan[1]

Abstract

The cerebellum is known to influence cerebral cortical activity via cerebello-thalamo-cortical (CTC) circuits and thereby may be implicated in the pathophysiology of multiple system atrophy (MSA). As the aim of this study, we investigated the abnormalities of corticocerebellar functional connectivity (FC) in patients with two variants of MSA. Resting-state functional magnetic resonance imaging (rs-fMRI) studies were obtained from 55 patients with MSA, including Parkinsonian (MSAp, $n = 29$) and cerebellar (MSAc, $n = 26$) variants. We also examined a similar number of healthy controls (HC, $n = 51$). Seed-based connectivity analysis was performed to assess alterations in CTC circuits. Relations between FC and clinical scores were assessed as well. Compared with the HC group, diminished FC was evident from bilateral dentate nucleus (DN) to motor cortex, bilateral basal ganglia, right cerebellum, default mode network (DMN), and limbic system in patients with MSAc. Patients with MSAp (vs HC subjects) showed less FC from left DN to right putamen, DMN, and limbic systems. Reduced FC was also demonstrated from left DN to DMN in patients with MSAc (vs MSAp), as well as from right DN to right cerebellum, DMN, basal ganglia, motor cortex, and limbic systems. In addition, the extent of FC from right DN to right cerebellum negatively correlated with Unified Parkinson's Disease Rating Scale-III scores in patients with MSA, while showing a positive association with Montreal Cognitive Assessment scores. The FC of DN was similarly altered in patients with MSAc and MSAp, although right cerebellar and motor cortical changes were more widespread in the MSAc group. There may be differing mechanisms of cerebellar functional activity responsible for motor and cognitive impairment, which should be further investigated.

Keywords Cerebellum · Dentate nucleus · Functional connectivity · Resting-state fMRI · Cerebello–thalamo-cortical (CTC) pathway

Introduction

Multiple system atrophy (MSA) is a sporadic, adult-onset neurodegenerative disease characterized by autonomic failure, pyramidal signs, parkinsonism, and symptoms of cerebellar ataxia. The parkinsonian (MSAp) and cerebellar (MSAc) subtypes of MSA are primarily motor disorders with many symptoms in common (motor and non-motor) (Gilman et al. 2008). However, MSAp is associated with more rapid functional deterioration, and the prognosis is poorer (Fanciulli and Wenning 2015), underscoring the importance of clinically separating these conditions. Studies have shown that abnormal glial cytoplasmic inclusions (GCIs) within nigrostriatal and/or olivopontocerebellar systems may indirectly contribute to dysfunction of striato-pallido-thalamo-cortical (STC) and cerebello-thalamo-cortical (CTC) pathways in patients with MSA (Su et al. 2001). Still, the pathophysiologic underpinnings are unclear, offering no real basis as yet for differentiating these MSA variants.

Given its anatomic and functional connectivity (FC) to the basal ganglia, forming part of the CTC circuit, the cerebellum has become a major investigative focus in this setting (Rosskopf et al. 2018; Wang et al. 2016; Wu and Hallett 2013). Findings of a semiquantitative postmortem analysis

HuaGuang Yang and Na Wang contributed equally to this work.

HuaGuang Yang and Na Wang are joint first author.

✉ GuoGuang Fan
  fanguog@sina.com

1 Department of Radiology, The First Affiliated Hospital of China Medical University, Shenyang, LN, China

2 Department of Neurology, The First Affiliated Hospital of China Medical University, Shenyang, LN, China

in patients with MSA ($N = 100$) have indicated that pathology within the basal ganglia and cerebellum, rather than pontine nucleus and inferior nucleus, seems to determine MSA subtype. Thus, the cerebellum may be pivotal in distinguishing MSAp from MSAc (Ozawa et al. 2004). Cerebellar gray matter in particular has shown significant volume reduction in patients with MSA, compared with healthy controls (HC); and this reduction was more pronounced in the MSAc (vs MSAp) subgroup (Minnerop et al. 2007). Moreover, Trace (D) may qualify as a quantitative marker for microstructural damage during the development of MSA. Its reported levels in cerebellum and in middle cerebellar peduncle were significantly reduced in patients with MSAc, relative to MSAp and HC group members (Pellecchia et al. 2011). In addition, a single-photon emission computed tomography, (SPECT) study has demonstrated a significant diminution in the cerebellar perfusion of patients with MSA (Cilia et al. 2005). These findings suggest that the cerebellum is subject to more extensive pathologic and microstructural alterations in the MSAc vs MSAp) variant. Although few studies have addressed cerebellar function in the context of MSA, changes in gray matter volume and perfusion undoubtedly influence cerebellar activity and reflect its functional status. These tentative differences in CTC circuitry and FC of MSA subtypes therefore merit further investigation.

Resting-state functional magnetic resonance imaging (rs-fMRI) is a powerful tool for mapping intrinsic cerebellar activity that is widely used to assess movement disorders (Biswal et al. 1995). The dentate nucleus (DN) is the largest deep nucleus in the human cerebellum. Signals from cerebellar outputs converge onto DN neurons, which then project to a distinct region of thalamus and innervate a specific area of cortex, thus completing the CTC circuit and influencing cortical function (Bostan et al. 2010). Accordingly, the DN may represent a region of interest (ROI) in exploring roles of the cerebellum. The DN is actually a common focus in studies of Parkinson's disease (PD) and its subtypes, consistently implicating compensatory cerebellar changes (Ballanger et al. 2008; Wu and Hallett 2013; Yu et al. 2007). A recent study has documented greater FC between DN and posterior cerebellar lobes in tremor-dominant than in non-tremor-dominant patients and in patients with PD than in HC subjects (Ma et al. 2015). However limited the studies of MSA may be in addressing cerebellar FC, MSA and PD exhibit the same dopamine pathology and motor symptoms, and a regional homogeneity study has confirmed localized abnormalities of motor cortical activity.

In this study, we used rs-fMRI to investigate cerebellar FC alterations in patients with MSA, examining FC between DN and regions of cortex or subcortical gray matter. We anticipated similarities and differences by disease subtype and expected that regional FC changes would correspond with clinically oriented assessments.

Materials and methods

Participants

The Institutional Review Board of China Medical University approved this investigation. Each subject granted informed consent after detailed briefing on the study protocol. All participants were right-handed, and none had contraindications for rs-fMRI. HC group members had no neurologic illnesses and no medical histories of neurosurgical procedures, substance abuse/dependence, endocrine disease, or thyroid disorders.

A total of 55 patients with MSA (MSAp, 29; MSAc, 26) and 51 HC subjects matched by age, sex, and educational level were recruited between February 2016 and June 2017. Using second consensus clinical criteria (Gilman et al. 2008), patients were diagnosed as probable MSA by the Department of Neurology at First Affiliated Hospital of China Medical University, Shenyang, China. HC recruits were solicited through community advertisement. All participants received antiparkinson medication ~12 h prior to rs-fMRI studies (ie, off-state scanning), and each underwent a battery of neuropsychologic tests, including the Montreal Cognitive Assessment (MoCA) and Hamilton Depression Scale (HAMD-24). Patients were assessed clinically using the Unified Parkinson's Disease Rating Scale (UPDRS-III) and staged via Hoehn and Yahr (H-Y) scale. HC candidates were excluded if the MoCA score was <26 (<25 at 12-years secondary education level) or the HAMD-24 score was >8.

Rs-fMRI image acquisition

Imaging data were generated using a 3.0 T MRI scanner (Magnetom Verio; Siemens, Erlangen, Germany) equipped with a 32-channel head coil at the Radiology Department of China Medical University. Subjects were awake but at rest, with eyes closed. Immediately following the scans, we routinely confirmed that none of the patients had fallen asleep.

Images were acquired through single, short gradient-echo echo-planar imaging sequences obtained in parallel and in anteroposterior commissural plane. The parameters were as follows: repetition time (TR), 2500 ms; echo time (TE), 30 ms; flip angle, 90°; slice number, 43; slice thickness, 3.5 mm without slice gap; field of view, 224×224 mm^2; matrix size, 64×64; and voxel size, $3.5 \times 3.5 \times 3.5$ mm. Three-dimensional T1-weighted images were obtained in sagittal orientation, employing a high-resolution three-dimensional sagittal magnetization-prepared rapid acquisition gradient echo sequence at the following parameters: TR, 5000 ms; TE, 2960 ms; field of view, 256×256 mm^2; matrix size, 256×256; flip angle, 12°; slice number, 176; slice thickness, 1 mm; distance factor, 0.5; and voxel size, $1.0 \times 1.0 \times 1.0$ mm.

Rs-fMRI data preprocessing

In conjunction with proprietary software (SPM8; http://www.fil.ion.ucl.ac.uk/spm), the Data Processing & Analysis for Brain Imaging (DPABI) toolbox (http://rfmri.org/dpabi) served to preprocess blood oxygen level dependent (BOLD) data. Magnetic saturation effects were avoided by discarding the first 10 images of each participant, processing the remainder as stipulated herein. Slice timing and head-motion correction were achieved by alignment with the first image of the session overall. On this basis, the following imaging features were grounds for exclusion: 1) >2.5 mm maximum displacement in any x, y, or z direction; 2) mean frame-wise displacement (FD, Jenkinson) > mean FD +2SD (standard deviation) 3) >2.5° of angular motion. Interactive reorientation and co-registration of functional and T1-weighted images were then performed as an optimization control measure. Information generated by new-segment algorithms (grey matter, white matter, and cerebrospinal fluid-tissue maps) was used for spatial normalization by DARTEL technique (Ashburner 2007). All images were spatially normalized to the DARTEL-Montreal Neurological Institute (MNI) space and resampled as $3 \times 3 \times 3$ mm^3 voxels. They were then smoothed using a Gaussian filter (6 mm) at full width and half maximum (FWHM). Subsequent preprocessing entailed removal of linear drift through linear regression and temporal band-pass filtering (0.01–0.08 Hz). Linear regression of head-motion parameters(mean FD, Jenkinson), global mean signals, white matter signals, and cerebrospinal fluid signals was needed to remove nuisance covariate effects (Biswal et al. 1995).

Defining regions of interest (ROIs)

Left and right DN ROIs were created using the WFU_PickAtlas (http://www.ansir.wfubmc.edu) (Fig. 1).
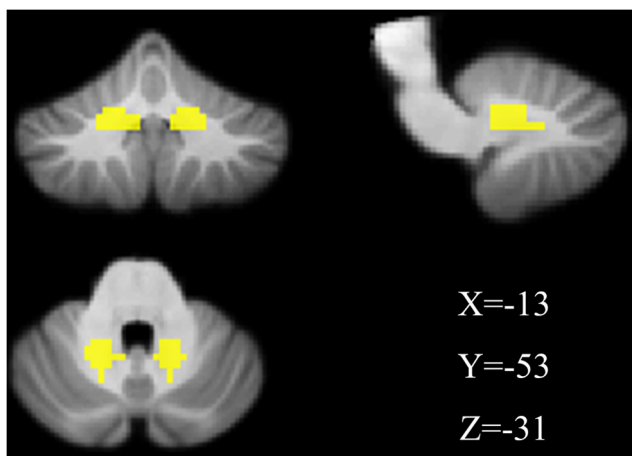

X=-13
Y=-53
Z=-31

Fig. 1 Seed region in the cerebellar dentate nucleus. View of the generated left and right (yellow) dentate nucleus superimposed to the spatially unbiased atlas template of the cerebellum and brainstem (Diedrichsen et al. 2009)

ROIs were then resliced into the MNI space. The BOLD time series of voxels within ROIs were averaged to generate corresponding reference time series. Using normalized T1-weighted high-resolution images, whole-brain masks were created for participants individually and stripped using BrainSuite2 (http://brainsuite.usc.edu). Only voxels within these masks were subject to further analysis.

FC analysis

Individual voxel-wise FC levels in ROIs were computed using DPABI software, extracting the average BOLD signal across a time series between bilateral DN seed references and whole brain in each subject. Correlation coefficients were ultimately converted to z-values (Fisher transformation) to achieve normality. For each subject, time series activation in seed regions served to predict activation elsewhere in the brain.

Statistical analyses

Various tests (one-way analysis of variance [ANOVA], chi-square, Kruskal-Wallis, Mann-Whitney, and two-sample *t*-test) were applied to assess demographic variables and clinical data, using standard software (SPSS v21.0; IBM, Armonk, NY, USA). Results were considered significant at $p < 0.05$.

FC data analysis relied on DPABI software. One-way ANOVA, using mean FD (Jenkinson),age, and sex as covariates, was engaged to examine FC differences among MSA-p, MSA-c, and HC groups (AlphaSim correction, $p < 0.01$; left: voxel size, 242; right: voxel size, 223). In post hoc analysis, we explored between-group FC differences within a mask, utilizing statistically significant ANOVA results and shared similar covariates for multiple comparison correction in ANOVA (MSA-p vs HC, MSA-c vs HC, MSA-p vs MSA-c; AlphaSim correction, $p < 0.01$).

The Spearman rank-order correlation was invoked for preliminary nonparametric analysis (via SPSS), investigating relations between UPDRS-III, International Cooperative Ataxia Rating Scale (ICARS), MoCA, and HAMD-24 scores, and FC levels in MSA groups. Significance was set at $p < 0.05$.

Results

Demographic and clinical data

There were no significant group-wise differences in age [F = 1.84; $p = 0.16$]; sex ($\chi 2 = 0.34$; $p = 0.56$), or years of education [F = 1.89; $p = 0.16$] (Table 1). As expected, the MSAp and MSAc groups showed significantly lower MoCA scores ($\chi 2 = 91.53$; $p = 0.000*$) and higher HAMD-24 scores ($\chi 2 = 90.15$; $p = 0.000*$) than the HC group, but were otherwise similar. There were no significant differences in duration of

Table 1 Demographic and clinical characteristics

Characteristics (Mean ± SD)	Control ($n = 51$)	MSAp ($n = 29$)	MSAc ($n = 26$)	F/$\chi2$	P value
age(years)	64.8 ± 3.77	62.41 ± 8.87	65.3 ± 6.88	1.84	0.16
Gender(male:femal)	23:28	13:16	14:12	0.34	0.56
Education	11.90 ± 2.55	10.76 ± 3.36	10.84 ± 3.99	1.89	0.16
Disease duration	N	3.28 ± 2.10	3.50 ± 1.58	318	0.32
UPDRS- III score	N	37.21 ± 21.22	31.29 ± 16.47	319	0.33
Hoehn and Yahr	N	2.69 ± 1.17	2.62 ± 1.09	357	0.74
MOCA score	26.73 ± 1.31	21.04 ± 4.08	21.24 ± 4.51	91.53	0.000*
HAMD score	1.94 ± 2.58	11.41 ± 5.85	10.58 ± 8.38	90.15	0.000*
ICARS	N	26.08 ± 12.73	45.14 ± 18.12	31.16	0.000*

SD standard deviation, *MSA* multiple system atrophy, *MSAp* MSAparkinsonian variant, *MSAc* MSAcerebellar variant, *HC* healthy controls, *UPDRS-III* Unified Parkinson's Disease Rating Scale, *MoCA* Montreal Cognitive Assessment, *HAMD* Hamilton Depression Scale

ICARS: International Cooperative Ataxia Scale Rating; 0.000*: values less than 0.000; $p < 0.05$ was considered statistically significant

illness (U = 318; $p = 0.66$), UPDRS-III score (U = 1.44; $p = 0.26$), or staging by H-Y scale ($\chi2 = 7.15$; $p = 0.15$).

Functional connectivity among MSAp, MSAc, and HC groups

Among the three groups, we found abnormalities in FC from bilateral DN to cerebellar, cortical, and subcortical regions, including right cerebellar VIII and Crus II, DMN (bilateral dorsolateral prefrontal cortex, bilateral inferior parietal lobe, bilateral precuneus, right middle temporal gyrus, bilateral cingulate cortex, and bilateral angular gyrus), motor cortex (bilateral precentral, bilateral postcentral, and bilateral supplementary motor areas [SMA]), basal ganglia (bilateral putamen, bilateral caudate, and bilateral thalamus), and limbic areas (bilateral insula, left parahippocampus, and bilateral hippocampus) (Table 2, Fig. 2).

Post hoc FC comparisons

Relative to HC group members, patients with MSAc showed extensively reduced FC from bilateral DN to right cerebellum (cerebellar VIII and Crus II), basal ganglia (bilateral caudate, right putamen, and bilateral thalamus), DMN (left dorsolateral prefrontal cortex, left inferior parietal lobe, bilateral precuneus, bilateral middle cingulate gyrus, bilateral middle temporal gyrus, and left angular gyrus) and right insula. Similarly, FC was diminished from left DN to DMN (right dorsolateral prefrontal cortex, left postcentral gurus, right parietal inferior lobe, and right angular gyrus) and limbic areas (right parahippocampus and right hippocampus), as well as from right DN to left putamen, bilateral SMA, DMN (bilateral precentral gyrus, left superior and inferior temporal gyrus, and left superior parietal lobe), left middle occipital cortex, left insula, and left amygdala (Table 3, Fig. 3).

Compared with the HC group, the MSAp group showed reduction in FC from left DN to right putamen; right insula; right parahippocampus; and right superior, middle, and inferior temporal lobe (Table 4, Fig. 4).

In comparing MSA subtypes, the MSAc group showed diminished FC from left DN to DMN (right superior frontal gyrus, right frontal middle gyrus, bilateral precuneus, and middle cingulate cortex) and from right DN to right cerebellum (cerebellar VIII and Crus II), DMN (left superior frontal gyrus, bilateral superior and middle temporal gyrus, right inferior temporal gyrus, bilateral precuneus), basal ganglia (right putamen, bilateral caudate, bilateral thalamus), left postcentral gyrus, left SMA, and right insula (Table 5, Fig. 5).

Correlation between neuropsychologic assessment and extent of FC

In MSA subtypes, an inverse correlation was identified between UPDRS-III scores and diminished right DN to right cerebellar FC ($r = -0.45$; $p = 0.000$) (Fig. 6a); whereas the FC of right DN to right cerebellum positively correlated with MoCA scores ($r = 0.33$; $p = 0.013$) (Fig. 6b). Declines in FC from right DN to cerebellum negatively correlated with ICARS scores ($r = -0.525$; $p = 0.000*$) (Fig. 6c), but no significant associations between HAMD-24 scores and extent of FC were evident.

Discussion

To our knowledge, this was the first published study to explore FC alterations of DN in the two motor subtypes of MSA. There are several major findings as a result. First, FC declines from DN to regions of cortex or subcortical gray matter appear similar for both MSAc and MSAp variants in terms of basal ganglia, DMN, and limbic systems, although more

Table 2 Brain regions with bilateral DN FC differences among the MSAp, MSAc, and HC groups

Brain regions	Hem	Voxels	MNI coordinate			t value	BA
			X	Y	Z		
Left dentate nucleus							
Cerebellum_VIII (aal)	R	120	30	−60	−56	9.28	NA
Cerebellum_Crus II (aal)	R	109	44	−65	−42	12.07	NA
Superior frontal gyrus (aal)	L/R	134/221	−20/20	45/44	39/41	7.59/8.73	BA9
Middle frontal gyrus (aal)	L/R	286/394	−35/25	32/40	39	7.93/7.12	BA46
Superior temporal gyrus (aal)	R	322	61	−44	14	9.96	BA22
Middle temporal gyrus (aal)	R	453	54	−3	−21	14.63	BA21
Inferior temporal gyrus (aal)	R	245	56	−12	−25	8.13	BA20
Superior parietal lobe (aal)	L/R	30/86	−36/37	−67/−57	52/55	6.02/8.01	BA40
Inferior parietal lobe (aal)	L/R	265/171	−39/43	−56/−57	53/51	9.00/9.93	BA40
Precuneus (aal)	L/R	447/443	−6/5	−63/−53	50/39	8.59/11.39	NA
Middle cingulum cortex (aal)	L/R	162/101	−8/3	−34/−42	43/40	9.41/7.12	NA
Insula (aal)	R	222	36	15	−12	15.36	BA48
Angular (aal)	L/R	156/304	−51/51	−65/−58	27	7.28/11.95	BA39
Thalamus (aal)	L/R	95/125	−12/13	−18/−21	12	9.89/8.19	NA
Putamen (aal)	R	122	25	3	5	11.01	NA
Caudate (aal)	L/R	59/102	−13/12	14/12	11/10	8.20/9.43	NA
ParaHippocampal (aal)	R	96	24	−11	−25	9.48	BA36
Hippocampus (aal)	R	63	24	−12	−19	7.43	BA35
Supply motor area (aal)	R	34	9	−25	55	5.36	BA4
Right dentate nucleus							
Cerebellum_Crus II_R (aal)	R	288	45	−69	−42	13.92	NA
Cerebellum_VIII_R (aal)	R	171	24	−63	−56	9.53	NA
Superior frontal gyrus (aal)	L/R	190/26	−17/21	16/7	59/50	7.13/6.20	BA8
Middle frontal Gyrus (aal)	L	314	−28	29	47	5.43	BA9
Superior temporal gyrus (aal)	L/R	87/226	−58/56	−11/−33	11/16	7.55/9.19	BA48
Middle temporal gyrus (aal)	L/R	126/216	−57/60	−44/−40	14/12	5.46/8.57	BA22
Inferior temporal gyrus (aal)	L/R	226/131	−45/45	−11/−15	−36/−32	11.35/13.17	BA20
Supply motor area (aal)	L/R	156/80	−3/7	23/19	51/56	5.81/8.00	BA6
Superior parietal lobe (aal)	L	68	−35	−65	51	6.76	BA7
Inferior parietal lobe (aal)	L	330	−40	−51	52	11.07	BA40
Middle Occipital lobe (aal)	L	153	−37	−86	12	6.89	BA19
Middle Cingulum cortex (aal)	L/R	42/54	−9/9	17/23	42/39	6.78/8.36	BA32
Insula (aal)	L/R	93/202	−38/47	−12/−9	−3/7	11.50/7.91	BA48
Precuneus (aal)	L/R	288/166	−3/1	−57/−52	42/35	6.45/6.50	NA
Angular (aal)	L	63	−43	−60	51	7.99	BA39
Putamen (aal)	L/R	33/145	−32/28	−11/10	−2/−6	8.07/8.33	BA48
Thalamus (aal)	L/R	122/144	−8/12	−22/−26	7/4	6.77/10.73	NA
Caudate (aal)	L/R	81/100	−9/10	8/11	11/13	11.00/8.86	NA
Precentral (aal)	L/R	36/177	−43/44	11/−8	49/55	7.41/6.55	BA9
Postcentral (aal)	L/R	61/119	−50/43	−29/−11	56/36	5.76/5.77	BA1
ParaHippocampal (aal)	L	41	−22	−13	−25	8.45	BA36
Hippocampus	L/R	31/19	−25/27	−7/−6	−25/−26	6.03/5.30	BA36

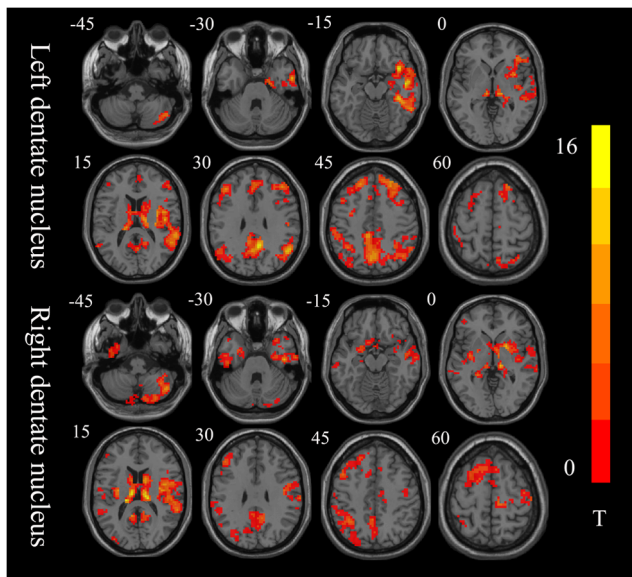*R* right, *L* left, *Hem* Hemisphere, *BA* Brodmann area

Fig. 2 Brain maps showing FC difference between the MSAp, MSAc and HC groups.. Differences were considered significant at $p < 0.01$ (AlphaSim correction). The left side of the image corresponds to the left side of the brain in axial orientation. Slice coordinates according to the MNI space are shown in the upper left corner of the slices, indicating the Z-axis in axial orientation

widespread changes of right cerebellum, DMN, basal ganglia, motor cortex, and limbic systems are more typical of patients with MSAc. Such findings improve our understanding of similarities and differences in clinical symptoms related to MSA subtypes. Furthermore, observed differences in BOLD signals largely suggest that cerebellar functional activity differs in these patient groups. The second major discovery is that diminished FC from left DN to right cerebellum negatively correlates with UPDRS-III scores and positively correlates with MoCA scores in both patient groups. The cerebellum is thus variably implicated in motor and cognitive deficits experienced by patients with MSA.

Pathologic studies have previously demonstrated that GCIs within the olivopontocerebellar system lead to CTC circuit dysfunction, a feature more apparent in patients with MSAc (Wenning et al. 1997). An increasing number of such studies also indicate that in patients with MSA, both primary and supplementary motor cortex is involved (Lantos 1998; Su et al. 2001; You et al. 2011). The cerebellum is particularly important for preparation and execution of movements (Purzner et al. 2007) and for their accurate timing (Dreher and Grafman 2002), given its intimate functional connections (via CTC circuits) to areas of cerebral motor cortex. Hence, dysfunction of CTC circuitry is a factor as well in deteriorating motor performance.

The DN is the largest site for bilateral hemispheric convergence of cerebellar information, which cerebral cortex then receives. Consequently, abnormalities of DN FC impose changes in output of cerebellar information (Middleton and

Strick 2000). During the present study, our patients with MSAc exhibited disruption of FC from bilateral DN to basal ganglia (bilateral putamen, bilateral caudate nucleus, and bilateral thalamus), motor cortex (bilateral postcentral gyrus, bilateral SMA, and bilateral precentral gyrus), and right cerebellum, compared with HC subjects. These results are consistent with earlier pathologic research findings and implicate the cerebellum (via CTC circuits) in the motor impairment of patients with MSAc (Su et al. 2001). Aside from past emphasis on nigrostriatal GCIs, which are prominent in the basal ganglia of patients with MSAp (Ozawa et al. 2004; Su et al. 2001), other imaging studies have identified putaminal atrophy and iron deposition as presumptive biomarkers for differentiating MSA subtypes (Lee et al. 2015). However, we found significantly less FC from DN to basal ganglia in patients with MSAp, suggesting dysfunction of the STC loop. In patients with MSAc, it is the olivopontocerebellar (rather than nigrostriatal) system that is profoundly degenerative. Even so, both systems may be affected as the disease advances. Most patients in our study qualified as early and middle stages, perhaps explaining why we observed diminished DN-to-cerebellum FC in the MSAc group only.

A growing body of evidence suggests that the cerebellum is involved not only in movement coordination (França et al. 2017; O'Callaghan et al. 2016; Sokolov et al. 2017; Wu and Hallett 2013) but also in regulation of cognitive function. Indeed, the cerebellum may be divided into cognitive- and motor-specific functional subregions (Sokolov et al. 2017). Although movement disorders are cardinal symptoms of patients with MSA, cumulative data indicate that cognitive impairment exists in both MSA subtypes (Barcelos et al., 2017; Kawai et al. 2008; Stankovic et al. 2014). According to our results, DN-to-cerebellum FC negatively correlates with UPDRS-III and ICARS scores but positively correlates with MoCA scores in patients with MSA. Many earlier studies have fostered the concept that enhanced resting-state cerebellar activity in patients with PD compensates for the dysfunctional STC circuits brought on by dopaminergic decline (Liu et al. 2013; Ma et al. 2015; Sen et al. 2010). However, it is unclear whether altered DN-to-cerebellum FC is compensatory or pathologic in this setting. Recently, it has been reported that in patients with PD, resting-state FC may be affected by dopaminergic drugs (O'Callaghan et al. 2016). Although the present investigation entailed off-state examinations, some effects of anti-Parkinson medications may have persistent in our patients, for whom the average disease duration was 3.39 years. FC may have been improved as a result, while still falling below that of the HC group. Despite overlap in many PD- and MSA-related symptoms (motor or non-motor in nature), disease progression is more rapid, and life expectancy is shorter in patients with MSA (Wenning et al. 1994). Furthermore, it is generally acknowledged that the pathologic underpinnings of these two diseases are not identical. MSA is

Table 3 Brain regions with significant FC differences between the MSAc and HC groups

Brain region	Hem	Voxels	MNI coordinate			t value	BA
			X	Y	Z		
Left Dentate nucleus							
MSAc-HC							
Cerebellum_VIII_R (aal)	R	120	30	−64	−56	−3.76	NA
Cerebellum_Crus II_R (aal)	R	109	45	−63	−42	−4.62	NA
Superior frontal gyrus (aal)	L/R	134/220	−16/20	42/46	43/39	3.97/−3.78	BA9
Middle frontal gyrus (aal)	L/R	286/394	−38/39	30/38	37/34	−4.83/−4.20	BA46
Superior temporal gyrus (aal)	R	303	52	−42	17	−3.71	BA42
Middle temporal gyrus (aal)	L/R	65/449	−51/52	−64/−56	24/16	−4.00/−3.45	BA21
Inferior temporal gyrus (aal)	R	245	52	−14	−24	−3.55	BA20
Parietal inferior lobe (aal)	L/R	265/165	−53/44	−30/−57	46/52	−4.53/−4.36	BA2/BA39
Precuneus (aal)	L/R	436/442	−6/5	−56/−52	48/37	−3.85/−4.54	NA
Middle cingulum gyrus (aal)	L/R	162/101	−8/10	−38/−48	44/36	−4.46/4.30	NA
Angular (aal)	L/R	156/304	−46/51	−61/−60	34	−3.45/−4.22	BA39
Insula (aal)	R	200	43	−7	13	−4.23	NA
Rolandic_Oper_R (aal)	R	138	42	−1	14	−4.12	BA48
Thalamus (aal)	L/R	121/92	−10/14	−23/−22	11/7	−3.50/−3.27	NA
Putamen (aal)	R	121	29	10	−3	−3.84	BA48
Caudate (aal)	L/R	44/102	−10/14	11/10	9/10	−4.27/−4.97	NA
ParaHippocampal(aal)	R	91	20	−8	−28	−3.64	BA36
Hippocampus (aal)	R	54	24	−13	−20	−3.46	BA35
Postcentral (aal)	L	42	−52	−29	54	−3.41	BA2
Right Dentate nucleus							
MSAc-HC							
Cerebellum_Crus II_R (aal)	R	287	40	−65	−46	−3.92	NA
Cerebellum_VIII_R (aal)	R	171	31	−64	−58	−3.55	NA
Superior frontal gyrus (aal)	L	190	−16	16	61	−3.36	BA8
Middle frontal gyrus (aal)	L	313	−54	−63	22	−3.51	BA39
Superior temporal gyrus (aal)	L/R	84/219	50/−59	−23/−49	16/19	−4.13/−3.44	BA48/BA22
Middle temporal gyrus (aal)	L/R	123/210	−59/60	−52/−42	20/12	−3.42/−4.32	BA22/BA42
Inferior temporal gyrus (aal)	L/R	224/131	−46/45	−14/−12	−34/−33	−4.48/−4.42	BA20
Parietal superior lobe (aal)	L	68	−33	−53	58	−3.19	BA40
Parietal inferior lobe (aal)	L	328	−43	−52	50	−4.43	BA40
Middle occipital cortex (aal)	L	153	−30	−85	22	−3.19	BA19
Middle cingulum gyrus (aal)	L/R	42/54	−6/9	−41/−15	51/50	−3.59/−3.40	NA
Precuneus (aal)	L/R	279/166	−3/3	−51/−52	46/36	−4.11/−3.10	BA23
Insula (aal)	L/R	93/279	−38/40	−8/−6	7/6	−3.40/−4.00	BA48
Putamen (aal)	L/R	33/145	−27/23	0/7	−5/1	−3.14/−4.65	BA48
Caudate (aal)	L/R	81/100	−12/14	11/10	10/7	−5.26/−4.13	NA
Thalamus (aal)	L/R	121/137	−9/13	−23/−26	7/1	−3.37/−4.38	NA
ParaHippocampal (aal)	L	41	−22	−7	−27	−3.76	BA36
Amygdala (aal)	L	22	30	0	−13	−3.62	BA34
Angular (aal)	L	63	−54	−64	26	−3.37	BA39
Precentral (aal)	L/R	36/177	−44/39	11/−11	46/58	−3.67/−4.04	BA6
Postcentral (aal)	L/R	56/119	−54/43	−15/−8	50/34	−2.98/−3.52	BA4
Supply Motor Area (aal)	L/R	156/80	−6/6	17/19	56/58	−3.91/−4.36	BA6

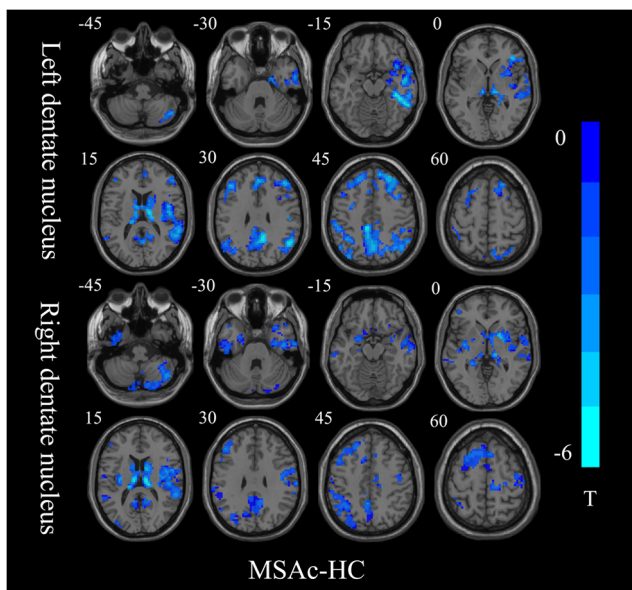*R* right, *L* left, *Hem* Hemisphere, *BA* Brodmann area

Fig. 3 Brain maps for FC difference between the MSAc and HC groups. Blue color denotes decreased FC in MSAc than HC group. Differences were considered significant at a threshold of $p < 0.01$, corrected via AlphaSim correction. The left side of the image corresponds to the left side of the brain in axial orientation; slice coordinates according to the MNI space are shown in the upper left corner of the slices, indicating Z-axis in axial orientation

Fig. 4 Statistical parametric map showing the significant differences in the DN FC between two groups: MSAp and HC. The threshold for display was set to $P < 0.01$, AlphaSim corrected; Slice coordinates according to the MNI space are shown in the upper left corner of the slices, T-value scale is to the right of the image

characterized by accumulations of -synuclein fibrils and GCIs in oligodendrocytes, whereas neuronal cytoplasmic Lewy bodies are hallmarks of PD. On the other hand, both MSA and PD represent -synuclein diseases (Dickson 2012). Previous FC studies conducted in patients with PD have concluded that cerebellar damage spawns regulatory dysfunction of motor and cognitive functions through compensatory mechanisms (Liu et al. 2013; Ma et al. 2015). In MSA, distinct functional disturbances are attached to various early pathologic changes. Thus, the negative correlation resulting from our analysis may signify differences in cerebellar functional activity that warrant further research. Remarkably, we did find significant correlations between abnormal right DN-to-
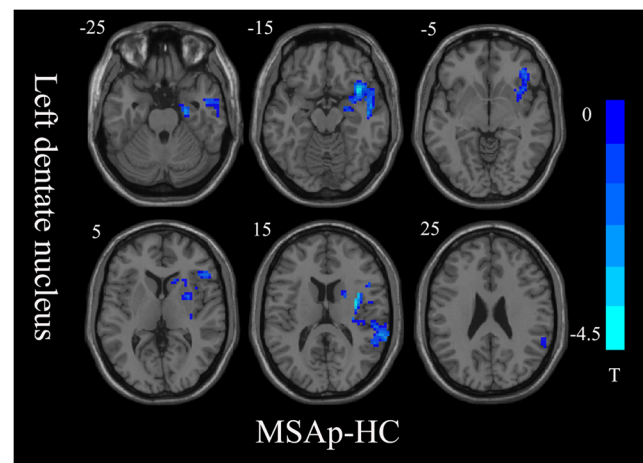
cerebellum FC patterns and ICARS scores, which is not necessarily surprising. As MSA evolves, one-third to one-half or more of all patients will present with cerebellar signs (Wenning et al. 1996). Although the ICARS was primarily designed to address pure cerebellar disorders (Trouillas et al. 1997), it has proved more useful than the UPDRS for extracting and rating the severity of cerebellar signs in patients with MSA (Tison et al. 2002). Shifts in both ICARS scores and UPDRS assessment further confirm that abnormal cerebellar function may figure prominently in MSA-related movement impairment.

The DMN seems to exhibit a high metabolic rate and embodies higher cognitive functions, such as action, cognition, emotion, interoception, and perception (Andrews-Hanna et al. 2010; Buckner et al. 2008). Several resting-state FC studies have shown that the cerebellum participates in higher-order networks of this sort (Buckner et al. 2011; Habas et al. 2009; Krienen and Buckner 2009). In the present study, disrupted FC from DN to DMN (posterior cingulate cortex, medial

Table 4 Brain regions with significant FC differences between the MSAp and HC groups

Brain regions	Hem	Voxels	MNI coordinate			t value	BA
			X	Y	Z		
Left Dentate nucleus							
MSAp<Normal							
Insula (aal)	R	122	36	15	−12	−4.70	BA48
Superior Temporal gyrus (aal)	R	115	55	−45	17	−2.88	BA22
Middle Temporal gyrus (aal)	R	76	50	−12	−12	−3.32	BA22
Inferior temporal gyrus (aal)	R	23	61	−8	−26	−3.12	BA21
Putamen (aal)	R	58	32	0	12	−3.99	BA48
ParaHippocampal (aal)	R	34	27	−12	−26	−424	BA36

R right, *L* left, *Hem* Hemisphere, *BA* Brodmann area

Table 5 Brain regions with significant FC differences between the MSAc and MSAp groups

Brain regions	Hem	Voxels	MNI coordinate			t value	BA
			X	Y	Z		
Left dentate nucleus							
MSAc-MSAp							
Superior frontal gyrus (aal)	R	123	20	34	50	−2.99	BA9
Middle frontal gyrus (aal)	R	67	32	30	50	−3.04	BA9
Precuneus (aal)	L/R	372/260	−8/6	−66/−64	50/46	−2.75/−3.49	BA7
Middle cingulum cortex (aal)	L/R	85/44	−6/3	−38/−38	41/36	−2.54/−2.67	BA23
Right dentate nucleus							
MSAc-MSAp							
Cerebellum_Crus II (aal)	R	242	45	−66	−39	−5.35	NA
Cerebellum_VIII (aal)	R	72	15	−71	−52	−3.62	NA
Superior frontal gyrus (aal)	L	74	−14	21	58	−2.49	BA8
Superior temporal gyrus (aal)	L/R	36/147	−59/57	−43/−37	21/17	−2.98/−2.95	BA42
Middle temporal gyrus (aal)	L/R	64/86	−58/58	−38/−45	6/11	−2.78/−2.89	BA22
Inferior temporal gyrus (aal)	R	46	45	−15	−32	−3.80	BA20
Inferior parietal lobe (aal)	L	225	−40	−49	55	−3.90	BA40
Precuneus (aal)	L/R	239/144	−5/5	−65/−56	42/42	−3.86/−2.87	BA7
Rolandic_Oper_R (aal)	R	205	45	−12	17	−3.25	BA48
Insula (aal)	R	85	40	−7	7	−3.73	BA48
Thalamus(aal)	L/R	115/108	−8/10	−18/−23	11/7	−3.95/−3.89	NA
Putamen (aal)	R	67	31	2	1	−2.77	BA48
Caudate (aal)	L/R	28/45	−8/12	4/6	12/11	−3.17/−3.55	NA
Postcentral (aal)	L	24	−52	−26	55	−3.15	BA3
Supply motor area (aal)	L	127	−10	17	61	−3.33	BA6

R right, *L* lef, *Hem* Hemisphere, *BA* Brodmann area

prefrontal cortex, inferior parietal lobe, and bilateral temporoparietal regions) was apparent in both patient groups, although not in HC subjects. Consistent with previous studies, these outcomes suggest that diminished DN connectivity

Fig. 5 Significant differences in left and right DN functional connectivity between MSAp and MSAc patients. Significant thresholds were corrected using AlphaSim correction and set at $p < 0.01$. Note that the left side corresponds to the right hemisphere

incites FC network neuromodulation and may contribute to the fundamental pathology of MSA. (Liu et al. 2013; O'Callaghan et al. 2016). Synchronous deactivation of cerebellum-to-DMN FC may explain the overlapping clinical symptoms in both patient groups. However, another study has described an augmentation of FC from left DN to DMN in patients with MSAp (vs HC subjects) (Franciotti et al. 2015) that may reflect differing participant characteristics, such as H-Y stage and sample size.

Depression, anxiety, and mild cognitive deficits are common symptoms and may precede the onset of motor impairment in patients with MSA (Benrud-Larson et al. 2005; Colosimo 2011; Ghorayeb et al. 2002). There is evidence that the limbic system (not cerebellum alone) is important in regulating emotion and cognition (Shao et al. 2015). In comparing each MSA patient group (MSAc or MSAp) with HC subjects, we encountered disrupted FC from DN to limbic system, including amygdala, insula, hippocampus, and parahippocampal gyrus. Of note, no significant associations between HAMD-24 scores and extent of FC were apparent. One possible explanation is that the limbic system supports a variety of functions, including emotion, behavior, motivation, long-term memory, and olfaction. HAMD-24 scoring helps gauge the severity of depression, but it is not directed at limbic functions as a whole (Chang et al. 2009; Lee et al. 2016). Underlying cerebellum-to-limbic FC must, therefore, be explored using a more detailed assessment scale. Still, These results herein suggest that limbic and cerebellar involvement
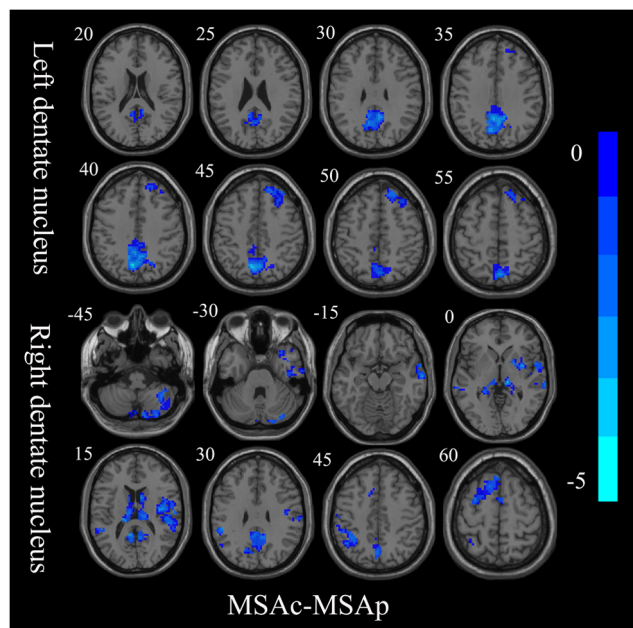
Fig. 6 Correlations between FC and motor and cognition scores. **a** UPDRS-III scores were negatively correlated with impaired connectivity between the right DN and right cerebellum in the MSA group. **b** MoCA scores were positively correlated with impaired connectivity between the right DN and right cerebellum in the MSA group. **c** Scatter plot of ICARS scores and impaired functional connectivity (FC) between the right dentate nucleus (DN) and right cerebellum
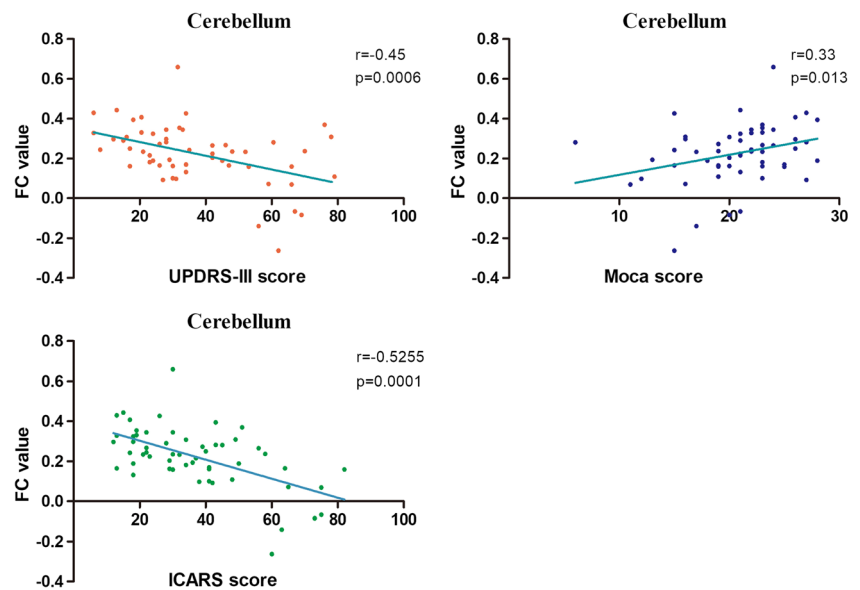
may account for non-motor symptoms, such as emotional and cognitive processing changes, found in the two variants of MSA.

In patients with MSAc (vs MSAp), more widespread alterations of FC were observed in limbic areas, accurately reflecting the ongoing pathology (Wenning et al. 1994). Other studies have also shown that extensively altered FC in the limbic system is uncommon in patients with shorter courses of MSA (Wang et al. 2017; Yao et al. 2017) but unequivocal in those with more protracted illness (Brenneis et al. 2003; Piao et al. 2001). One previous study has reported that the volume of insular gray matter declined in patients with MSAp and mean disease duration <5 years (Shao et al. 2015). Pathologic research has further documented temporal lobe atrophy in conjunction with GCIs, with neuronal cytoplasmic inclusions confined to limbic system, especially in cases of long-term MSA (Piao et al. 2001; Shibuya et al. 2000). However, our patient population was in relatively early stages of the disease (average disease duration: MSAp, 3.28 years; MSAc, 3.50 years). Although previous efforts have routinely focused on structural and pathologic changes, FC alterations may precede such morphologic developments (Brenneis et al. 2003; Tir et al. 2009; Wenning et al. 1994).

At present, there have been three other published studies of subcortical network FC in patients with MSA: 1) Chou et al. (Chou et al. 2015) found significant changes in cerebellum-to-cerebrum FC networks after repetitive transcranial magnetic stimulation; 2) Rosskopf et al. (Rosskopf et al. 2018) demonstrated a hyperconnective pontocerebellar network but a hypoconnective DMN; and 3) Yao and colleagues et (Yao et al. 2017) reported

declines in FC networks from bilateral cerebellar DN to frontal or motor cortex in patients with MSAp. In our investigation, aimed at cerebellum-to-cortex FC abnormalities due to MSA, both MSAp and MSAc variants were marked by functional network deficits. The Rosskopf study seemed more focused on cortical FC network dysfunction, whereas we explored DN connectivity abnormalities and subsequent FC network neuromodulatioIn this regard, the study by Yao was more aligned, but itis still debatable whether the cerebellum plays a compensatory or pathologic role in patients with MSA. Our findings, as well as the corroborative cerebellar pathology, indicate that the FC of networks is altered in patients with MSA.

Asymmetric pathologic change is not unique in patients with MSA or PD (Brenneis et al. 2007; Brenneis et al. 2003; Tir et al. 2009). Asprevious studies have revealed, increased vulnerability of the right hemisphere todopaminergic denervation may contribute to such asymmetries (Sullivan and Szechtman 1995). In our study, FC deficits were more pronounced from left DN to right cerebral cortex; and FC from right DN to cerebral cortex was unaltered in patients with MSAp (relative to controls) The fact that primary reciprocal connections between the cerebral cortex and the cerebellar hemispheres are contralaterally organized (Brodal 1979), it is reasonable that the abnormal left DN-based FC network we witnessed may further contribute to hemispheric asymmetries within the realm of MSA.. However, the concept pathophysiologic lateralization in patients with MSAp has yet to be verified.

The present study has two major limitations. Our enrollment included patients with probable MSA, based on the

most stringent clinical criteria for diagnosis, but autopsy confirmation was lacking. Consequently, a bias in candidate selection cannot be excluded. Second, The cumulative effects of anti-Parkinson medications may also linger, affecting brain function, so future studies of this nature should involve drug-naïve patients.

In summary, our data suggest that patients with MSAp and MSAc share a diminution in FC from DN to basal ganglia, DMN, and limbic structures, whereas more widespread alterations of motor cortex and right cerebellum are largely confined to those with MSAc. These findings may improve our understanding of similarities and differences surrounding both disease subtypes. They also provide compelling evidence that the cerebellum is pivotal in the evolution of MSA, particularly with respect to MSAc. In general, however, the respective mechanisms of cerebellar functional activity accounting for motor and cognitive impairment may not be the same.

Compliance with ethical standards

Conflict of interest None.

Ethical approval All procedures used to evaluate human participants were performed in accord with institutional and/or national research committee ethical standards and with the 1964 Helsinki declaration (including later amendments) or comparable ethical standards.

Informed consent Each subject granted informed consent for study participation.

References

Andrews-Hanna, J. R., Reidler, J. S., Sepulcre, J., Poulin, R., & Buckner, R. L. (2010). Functional-anatomic fractionation of the brain's default network. *Neuron, 65*(4), 550-562.

Ashburner, J. (2007). A fast diffeomorphic image registration algorithm. *NeuroImage, 38*(1), 95–113.

Ballanger, B., Baraduc, P., Broussolle, E., Le, B. D., Desmurget, M., & Thobois, S. (2008). Motor urgency is mediated by the contralateral cerebellum in Parkinson's disease. *Journal of Neurology, Neurosurgery, and Psychiatry, 79*(10), 1110–1116.

Benrud-Larson, L. M., Sandroni, P., Schrag, A., & Low, P. A. (2005). Depressive symptoms and life satisfaction in patients with multiple system atrophy. *Movement Disorders: Official Journal of the Movement Disorder Society, 20*(8), 951–957.

Biswal, B., Yetkin, F. Z., Haughton, V. M., & Hyde, J. S. (1995). Functional connectivity in the motor cortex of resting human brain using echo-planar MRI. *Magnetic Resonance in Medicine, 34*(4), 537–541.

Bostan, A. C., Dum, R. P., & Strick, P. L. (2010). The basal ganglia communicate with the cerebellum. *Proceedings of the National Academy of Sciences of the United States of America, 107*(18), 8452–8456.

Brenneis, C., Seppi, K., Schocke, M. F., Müller, J., Luginger, E., Bösch, S., Löscher, W. N., Büchel, C., Poewe, W., & Wenning, G. K. (2003). Voxel-based morphometry detects cortical atrophy in the Parkinson variant of multiple system atrophy. *Movement*

Disorders: Official Journal of the Movement Disorder Society, 18*(10), 1132–1138.

Brenneis, C., Egger, K., Scherfler, C., Seppi, K., Schocke, M., Poewe, W., & Wenning, G. K. (2007). Progression of brain atrophy in multiple system atrophy. A longitudinal VBM study. *Journal of Neurology, 254*(2), 191–196.

Brodal, P. (1979). The pontocerebellar projection in the rhesus monkey: An experimental study with retrograde axonal transport of horseradish peroxidase. *Neuroscience, 4*(2), 193–208.

Buckner, R. L., Andrews-Hanna, J. R., & Schacter, D. L. (2008). The brain's default network: Anatomy, function, and relevance to disease. *Annals of the New York Academy of Sciences, 1124,* 1–38.

Buckner, R. L., Krienen, F. M., Castellanos, A., Diaz, J. C., & Yeo, B. T. (2011). The organization of the human cerebellum estimated by intrinsic functional connectivity. Journal of neurophysiology, 106(5), 2322-2345.

Chang, C. C., Chang, Y. Y., Chang, W. N., Lee, Y. C., Wang, Y. L., Lui, C. C., Huang, C. W., & Liu, W. L. (2009). Cognitive deficits in multiple system atrophy correlate with frontal atrophy and disease duration. *European Journal of Neurology, 16*(10), 1144–1150.

Chou, Y. H., You, H., Wang, H., Zhao, Y. P., Hou, B., Chen, N. K., & Feng, F. (2015). Effect of repetitive transcranial magnetic stimulation on fMRI resting-state connectivity in multiple system atrophy. *Brain Connectivity, 5*(7), 451–459.

Cilia, R., Marotta, G., Benti, R., Pezzoli, G., & Antonini, A. (2005). Brain SPECT imaging in multiple system atrophy. *Journal of Neural Transmission, 112*(12), 1635–1645.

Colosimo, C. (2011). Nonmotor presentations of multiple system atrophy. *Nature Reviews Neurology, 7*(5), 295–298.

Dickson, D. W. (2012). Parkinson's disease and parkinsonism: Neuropathology. *Cold Spring Harbor Perspectives in Medicine, 2*(8).

Diedrichsen, J., Balsters, J. H., Flavell, J., Cussans, E., & Ramnani, N. (2009). A probabilistic MR atlas of the human cerebellum. *NeuroImage, 46*(1), 39–46.

Dreher, J. C., & Grafman, J. (2002). The roles of the cerebellum and basal ganglia in timing and error prediction. *The European Journal of Neuroscience, 16*(8), 1609–1619.

Fanciulli, A., & Wenning, G. K. (2015). Multiple-system atrophy. *The New England Journal of Medicine, 372*(3), 249–263.

França, C., de Andrade, D. C., Teixeira, M. J., Galhardoni, R., Silva, V., Barbosa, E. R., et al. (2017). Effects of cerebellar neuromodulation in movement disorders: A systematic review. *Brain Stimulation, 11*(2), 249–260.

Franciotti, R., Delli, P. S., Perfetti, B., Tartaro, A., Bonanni, L., Thomas, A., et al. (2015). Default mode network links to visual hallucinations: A comparison between Parkinson's disease and multiple system atrophy. *Movement Disorders: Official Journal of the Movement Disorder Society, 30*(9), 1237–1247.

Ghorayeb, I., Yekhlef, F., Chrysostome, V., Balestre, E., Bioulac, B., & Tison, F. (2002). Sleep disorders and their determinants in multiple system atrophy. *Journal of Neurology, Neurosurgery, and Psychiatry, 72*(6), 798–800.

Gilman, S., Wenning, G. K., Low, P. A., Brooks, D. J., Mathias, C. J., Trojanowski, J. Q., Wood, N. W., Colosimo, C., Durr, A., Fowler, C. J., Kaufmann, H., Klockgether, T., Lees, A., Poewe, W., Quinn, N., Revesz, T., Robertson, D., Sandroni, P., Seppi, K., & Vidailhet, M. (2008). Second consensus statement on the diagnosis of multiple system atrophy. *Neurology, 71*(9), 670–676.

Habas, C., Kamdar, N., Nguyen, D., Prater, K., Beckmann, C. F., Menon, V., & Greicius, M. D. (2009). Distinct cerebellar contributions to intrinsic connectivity networks. *The Journal of Neuroscience: The Official Journal of the Society for Neuroscience, 29*(26), 8586–8594.

Kawai, Y., Suenaga, M., Takeda, A., Ito, M., Watanabe, H., Tanaka, F., Kato, K., Fukatsu, H., Naganawa, S., Kato, T., Ito, K., & Sobue, G. (2008). Cognitive impairments in multiple system atrophy: MSAC vs MSAP. *Neurology, 70*(16 Pt 2), 1390–1396.

Krienen, F. M., & Buckner, R. L. (2009). Segregated fronto-cerebellar circuits revealed by intrinsic functional connectivity. *Cerebral Cortex, 19*(10), 2485–2497.

Lantos, P. L. (1998). The definition of multiple system atrophy: A review of recent developments. *Journal of Neuropathology and Experimental Neurology, 57*(12), 1099–1111.

Lee, J. H., Kim, T. H., Mun, C. W., Kim, T. H., & Han, Y. H. (2015). Progression of subcortical atrophy and iron deposition in multiple system atrophy: A comparison between clinical subtypes. *Journal of Neurology, 262*(8), 1876–1882.

Lee, M. J., Shin, J. H., Seoung, J. K., Lee, J. H., Yoon, U., Oh, J. H., Jung, D. S., & Kim, E. J. (2016). Cognitive impairments associated with morphological changes in cortical and subcortical structures in multiple system atrophy of the cerebellar type. *European Journal of Neurology, 23*(1), 92–100.

Liu, H., Edmiston, E. K., Fan, G., Xu, K., Zhao, B., Shang, X., et al. (2013). Altered resting-state functional connectivity of the dentate nucleus in Parkinson's disease. *Psychiatry Research, 211*(1), 64–71.

Ma, H., Chen, H., Fang, J., Gao, L., Ma, L., Wu, T., Hou, Y., Zhang, J., & Feng, T. (2015). Resting-state functional connectivity of dentate nucleus is associated with tremor in Parkinson's disease. *Journal of Neurology, 262*(10), 2247–2256.

Middleton, F. A., & Strick, P. L. (2000). Basal ganglia and cerebellar loops: Motor and cognitive circuits. *Brain Research. Brain Research Reviews, 31*(2–3), 236–250.

Minnerop, M., Specht, K., Ruhlmann, J., Schimke, N., Abele, M., Weyer, A., Wüllner, U., & Klockgether, T. (2007). Voxel-based morphometry and voxel-based relaxometry in multiple system atrophy-a comparison between clinical subtypes and correlations with clinical parameters. *NeuroImage, 36*(4), 1086–1095.

O'Callaghan, C., Hornberger, M., Balsters, J. H., Halliday, G. M., Lewis, S. J., & Shine, J. M. (2016). Cerebellar atrophy in Parkinson's disease and its implication for network connectivity. *Brain: A Journal of Neurology, 139*(Pt 3), 845–855.

Ozawa, T., Paviour, D., Quinn, N. P., Josephs, K. A., Sangha, H., Kilford, L., et al. (2004). The spectrum of pathological involvement of the striatonigral and olivopontocerebellar systems in multiple system atrophy: Clinicopathological correlations. *Brain: A Journal of Neurology, 127*(Pt 12), 2657–2671.

Pellecchia, M. T., Barone, P., Vicidomini, C., Mollica, C., Salvatore, E., Ianniciello, M., Liuzzi, R., Longo, K., Picillo, M., de Michele, G., Filla, A., Brunetti, A., Salvatore, M., & Pappatà, S. (2011). Progression of striatal and extrastriatal degeneration in multiple system atrophy: A longitudinal diffusion-weighted MR study. *Movement Disorders: Official Journal of the Movement Disorder Society, 26*(7), 1303–1309.

Piao, Y. S., Hayashi, S., Hasegawa, M., Wakabayashi, K., Yamada, M., Yoshimoto, M., et al. (2001). Co-localization of alpha-synuclein and phosphorylated tau in neuronal and glial cytoplasmic inclusions in a patient with multiple system atrophy of long duration. *Acta Neuropathologica, 101*(3), 285–293.

Purzner, J., Paradiso, G. O., Cunic, D., Saint-Cyr, J. A., Hoque, T., Lozano, A. M., Lang, A. E., Moro, E., Hodaie, M., Mazzella, F., & Chen, R. (2007). Involvement of the basal ganglia and cerebellar motor pathways in the preparation of self-initiated and externally triggered movements in humans. *The Journal of Neuroscience: The Official Journal of the Society for Neuroscience, 27*(22), 6029–6036.

Rosskopf, J., Gorges, M., Müller, H. P., Pinkhardt, E. H., Ludolph, A. C., & Kassubek, J. (2018). Hyperconnective and hypoconnective cortical and subcortical functional networks in multiple system atrophy. *Parkinsonism & Related Disorders, 49*, 75–80.

Sen, S., Kawaguchi, A., Truong, Y., Lewis, M. M., & Huang, X. (2010). Dynamic changes in cerebello-thalamo-cortical motor circuitry during progression of Parkinson's disease. *Neuroscience, 166*(2), 712–719.

Shao, N., Yang, J., & Shang, H. (2015). Voxelwise meta-analysis of gray matter anomalies in Parkinson variant of multiple system atrophy

and Parkinson's disease using anatomic likelihood estimation. *Neuroscience Letters, 587*, 79–86.

Shibuya, K., Nagatomo, H., Iwabuchi, K., Inoue, M., Yagishita, S., & Itoh, Y. (2000). Asymmetrical temporal lobe atrophy with massive neuronal inclusions in multiple system atrophy. *Journal of the Neurological Sciences, 179*(S1-2), 50–58.

Sokolov, A. A., Miall, R. C., & Ivry, R. B. (2017). The cerebellum: Adaptive prediction for movement and cognition. *Trends in Cognitive Sciences, 21*(5), 313–332.

Stankovic, I., Krismer, F., Jesic, A., Antonini, A., Benke, T., Brown, R. G., Burn, D. J., Holton, J. L., Kaufmann, H., Kostic, V. S., Ling, H., Meissner, W. G., Poewe, W., Semnic, M., Seppi, K., Takeda, A., Weintraub, D., Wenning, G. K., & on behalf of the Movement Disorders Society MSA (MODIMSA) Study Group. (2014). Cognitive impairment in multiple system atrophy: A position statement by the neuropsychology task force of the MDS multiple system atrophy (MODIMSA) study group. *Movement Disorders: Official Journal of the Movement Disorder Society, 29*(7), 857–867.

Su, M., Yoshida, Y., Hirata, Y., Watahiki, Y., & Nagata, K. (2001). Primary involvement of the motor area in association with the nigrostriatal pathway in multiple system atrophy: Neuropathological and morphometric evaluations. *Acta Neuropathologica, 101*(1), 57–64.

Sullivan, R. M., & Szechtman, H. (1995). Asymmetrical influence of mesocortical dopamine depletion on stress ulcer development and subcortical dopamine systems in rats: Implications for psychopathology. *Neuroscience, 65*(3), 757–766.

Tir, M., Delmaire, C., Le, T. V., Duhamel, A., Destée, A., Pruvo, J. P., et al. (2009). Motor-related circuit dysfunction in MSAP: Usefulness of combined whole-brain imaging analysis. *Movement Disorders: Official Journal of the Movement Disorder Society, 24*(6), 863–870.

Tison, F., Yekhlef, F., Balestre, E., Chrysostome, V., Quinn, N., Wenning, G. K., et al. (2002). Application of the international cooperative Ataxia scale rating in multiple system atrophy. *Movement Disorders: Official Journal of the Movement Disorder Society, 17*(6), 1248–1254.

Trouillas, P., Takayanagi, T., Hallett, M., Currier, R. D., Subramony, S. H., Wessel, K., Bryer, A., Diener, H. C., Massaquoi, S., Gomez, C. M., Coutinho, P., Hamida, M. B., Campanella, G., Filla, A., Schut, L., Timann, D., Honnorat, J., Nighoghossian, N., & Manyam, B. (1997). International cooperative Ataxia rating scale for pharmacological assessment of the cerebellar syndrome. The Ataxia neuropharmacology Committee of the World Federation of neurology. *Journal of the Neurological Sciences, 145*(2), 205–211.

Wang, H., Li, L., Wu, T., Hou, B., Wu, S., Qiu, Y., Feng, F., & Cui, L. (2016). Increased cerebellar activation after repetitive transcranial magnetic stimulation over the primary motor cortex in patients with multiple system atrophy. *Annals of Translational Medicine, 4*(6), 103.

Wang, N., Edmiston, E. K., Luo, X., Yang, H., Chang, M., Wang, F., et al. (2017). Comparing abnormalities of amplitude of low-frequency fluctuations in multiple system atrophy and idiopathic Parkinson's disease measured with resting-state fMRI. *Psychiatry Research, 269*, 73–81.

Wenning, G. K., Ben, S. Y., Magalhães, M., Daniel, S. E., & Quinn, N. P. (1994). Clinical features and natural history of multiple system atrophy. An analysis of 100 cases. *Brain: A Journal of Neurology, 117*(Pt 4), 835–845.

Wenning, G. K., Tison, F., Elliott, L., Quinn, N. P., & Daniel, S. E. (1996). Olivopontocerebellar pathology in multiple system atrophy. *Movement Disorders: Official Journal of the Movement Disorder Society, 11*(2), 157–162.

Wenning, G. K., Tison, F., Ben, S. Y., Daniel, S. E., & Quinn, N. P. (1997). Multiple system atrophy: A review of 203 pathologically proven cases. *Movement Disorders: Official Journal of the Movement Disorder Society, 12*(2), 133–147.

Wu, T., & Hallett, M. (2013). The cerebellum in Parkinson's disease. *Brain: A Journal of Neurology, 136*(Pt 3), 696–709.

Yao, Q., Zhu, D., Li, F., Xiao, C., Lin, X., Huang, Q., et al. (2017). Altered functional and causal connectivity of Cerebello-cortical circuits between multiple system atrophy (parkinsonian type) and Parkinson's disease. *Frontiers in Aging Neuroscience, 9*, 266.

You, H., Wang, J., Wang, H., Zang, Y. F., Zheng, F. L., Meng, C. L., & Feng, F. (2011). Altered regional homogeneity in motor cortices in patients with multiple system atrophy. *Neuroscience Letters, 502*(1), 18–23.

Yu, H., Sternad, D., Corcos, D. M., & Vaillancourt, D. E. (2007). Role of hyperactive cerebellum and motor cortex in Parkinson's disease. *NeuroImage, 35*(1), 222–233.